3-D Numerical Model for Wave-Induced Seabed Response around an Offshore Pipeline

Zuodong Liang, Dong-Sheng Jeng

Abstract—Seabed instability around an offshore pipeline is one of key factors that need to be considered in the design of offshore infrastructures. Unlike previous investigations, a three-dimensional numerical model for the wave-induced soil response around an offshore pipeline is proposed in this paper. The numerical model was first validated with 2-D experimental data available in the literature. Then, a parametric study will be carried out to examine the effects of wave, seabed characteristics and confirmation of pipeline. Numerical examples demonstrate significant influence of wave obliquity on the wave-induced pore pressures and the resultant seabed liquefaction around the pipeline, which cannot be observed in 2-D numerical simulation.

Keywords—Pore pressure, 3D wave model, seabed liquefaction, pipeline.

I. INTRODUCTION

NOWADAYS, many offshore structures have been commonly constructed over the last few decades for the ever-increasing engineering activities in exploring the marine resource in the ocean. Submarine pipelines, as one of the popular offshore infrastructures, have been extensively used for transportation of natural gas and oil from offshore platform, and disposal of industrial as well as municipal waste. For guarantying the safety of usage of such submarine pipelines, the coastal engineers have to consider the unexpected load including the wave, current, and anchor dropping/dredging, which might induce the its stability and decrease its life span. Thus, it is customary to bury the pipeline by trenching and refilling soil whose cost is relatively high and time-consuming [1]–[3].

It is a rather complicated engineering problem to design a marine pipeline regrading to its stability. One of the vital factors that must be taken into account is the seabed stability in vicinity of a pipeline. When the flow pattern becomes complicated by the interference of ocean wave and current, the fluctuation of dynamic pressure will be generated on the sea floor. With the existence of considerable fluctuation, it will further induce the development of excess pore pressure within a porous seabed, which has been considered as a dominant index to evaluate the instability of seabed. More precisely, they penetrate into the porous medium and induce decrease of effective stress within the soil column until the soil can lose its strength in bearing any load resulting in horizontal shear failure and vertical liquefaction respectively [4]. Therefore, the evaluation of the soil response, including pore pressure, effective stresses and soil displacements,

is particularly important for marine geotechnical engineers involved in the design of offshore pipelines.

As repeated in the literature, two well-known main mechanisms of dynamic wave-induced seabed liquefactions are the momentary liquefaction and residual liquefaction based on in the field measurements and laboratory experiments [5]. The first mechanism, momentary liquefaction, can occur beneath wave trough when the great seepage flow is upward directly. Since this kind of liquefaction may be happen within a short duration as the passage of wave trough, it is also called instantaneous liquefaction. The other mechanism, residual liquefaction, takes place as a result from a compacted and cyclic shearing process that the build-up of excess pore pressure in the seabed [6]. As mention previously, the waves also can induce shear stress in the soil when the waves propagate, which has been analytically investigated [7], [8]. Whereas the wave-induced shear stress has less impact on seabed instability compared to that caused by the previous two mechanism above. However, in this study, the authors only focus on the first mechanism regrading to the wave-induced seabed instantaneous response.

Based on the performance in a wave flume with real waves or centrifuge test, some laboratory experiments were conducted to investigate the wave-induced seabed response and the stability of submarine pipelines [9]–[12]. The experiment indicated that the excessive seepage flow and the resulting piping are the major factor to cause the onset of scour beneath the pipeline. Additionally, the experimental results shown that the pipeline behaviour is mainly dependent on its gravity rather than the wave condition in case of liquefied seabed.

With the rapid development of computational technique and computing resource, numerical simulation on wave-seabed-structure interaction may be considered the most flexible approach, as it allows researchers to simulate large-scale and realistic models and to couple soil model with fluid. Different numerical methods, including finite element method (FEM), finite difference method (FDM) and boundary element method (BEM) [13]–[15] have been applied to simulate the dynamic wave-induced seabed response as well as seabed instability in the past. Later on, some FEM numerical models were built up for investigating a more complicated WSSI problem involving trenched pipeline or multi-layered and anisotropic seabed [16]–[18]. However, the aforementioned studies exist a main limitation that is the effect of linear or non-linear wave was evaluated from the analytical solutions. Consequently, these models may not be able to fully predict the seabed response around pipeline

Z. Liang and D. S. Jeng are with the School of Engineering, Griffith University, Parklands Drive Southport, QLD 4222, Australia (e-mail: zuodong.liang@griffithuni.edu.au).

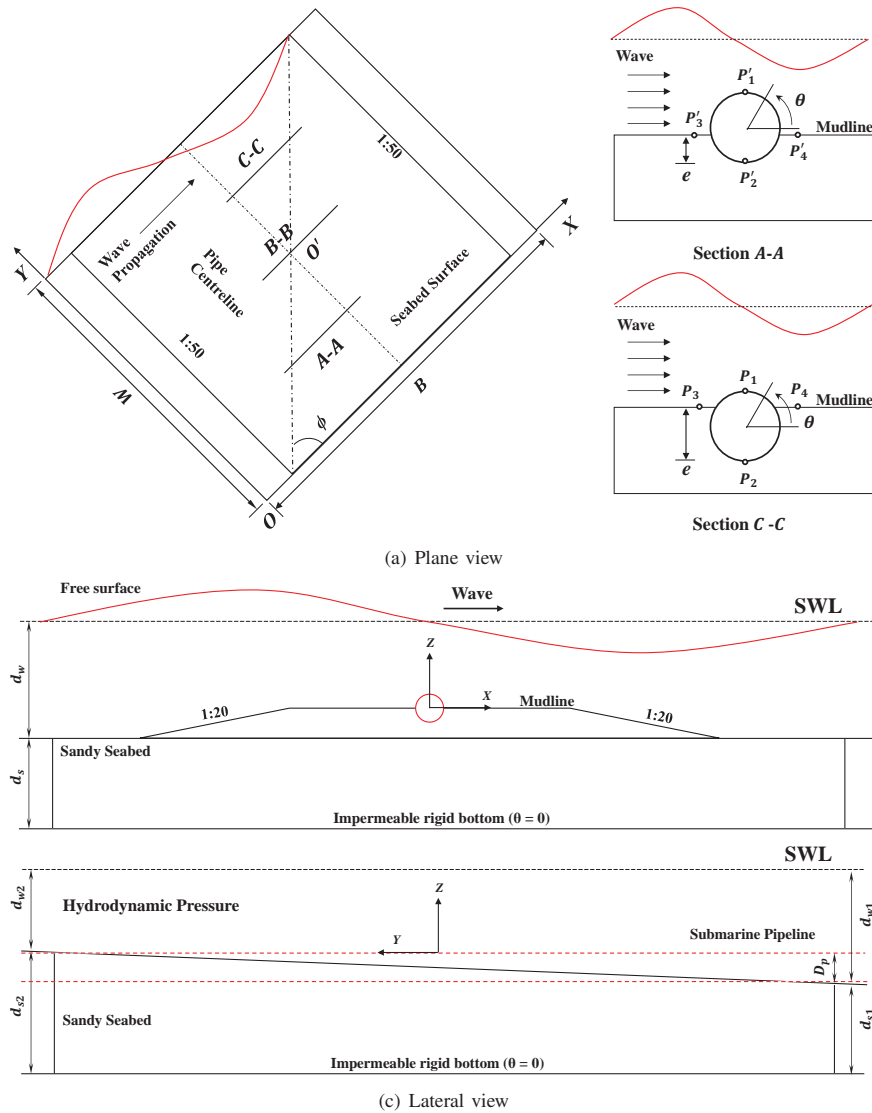(a) Plane view

(c) Lateral view

Fig. 1 Schematic graph of the computational domain addressed in this study

which is partly buried or mounted on a seabed. Later on, some numerical model have been proposed to remedy those limitations [19], [20]. But their numerical models are limited to a 2-D model due to the lack of 3-D wave model developed in COMSOL.

The purpose of this paper is to establish a three-dimensional integrated numerical model for transient soil components in the vicinity of the submarine pipeline under the progressive wave loading. In the wave model, the Reynolds-Averaged Navier-Stokes equation is solved to simulate the progressive wave motion over a porous seabed with a slope gradient. Moreover, a turbulent model is involved for describing the non-linear phenomenon. In the seabed model, the distribution of transient soil pressure in the vicinity of submarine pipeline is investigated by solving the Biot's consolidation equation within an elastic soil constitutive. The integrated numerical model is validated through comparison with published

analytical solution and experimental results. Finally, a series of parametric study is carried out for evaluating the effects of wave condition, seabed condition and the pipeline burial depth on the distribution of wave-induced oscillatory pore pressure in the vicinity of the submarine pipeline.

II. NUMERICAL MODEL

Fig. 1 shows the schematic diagram of present model in this study. The submarine pipeline with outer diameter (D_p) within a sloping porous seabed $(B \times W)$ is considered here. The fifth-order Stokes wave is generated with fixed water depth (d_w) propagates in the positive $x-$ direction from left to right, while $z-$ direction is upward from the impermeable bottom of the porous seabed. Besides, the slope gradient (α) of porous seabed is along the $y-$ direction. The wave incident angle (ϕ) is defined as the intersection angle between the direction of progressive wave and $x-$ axis. All the wave characteristics,
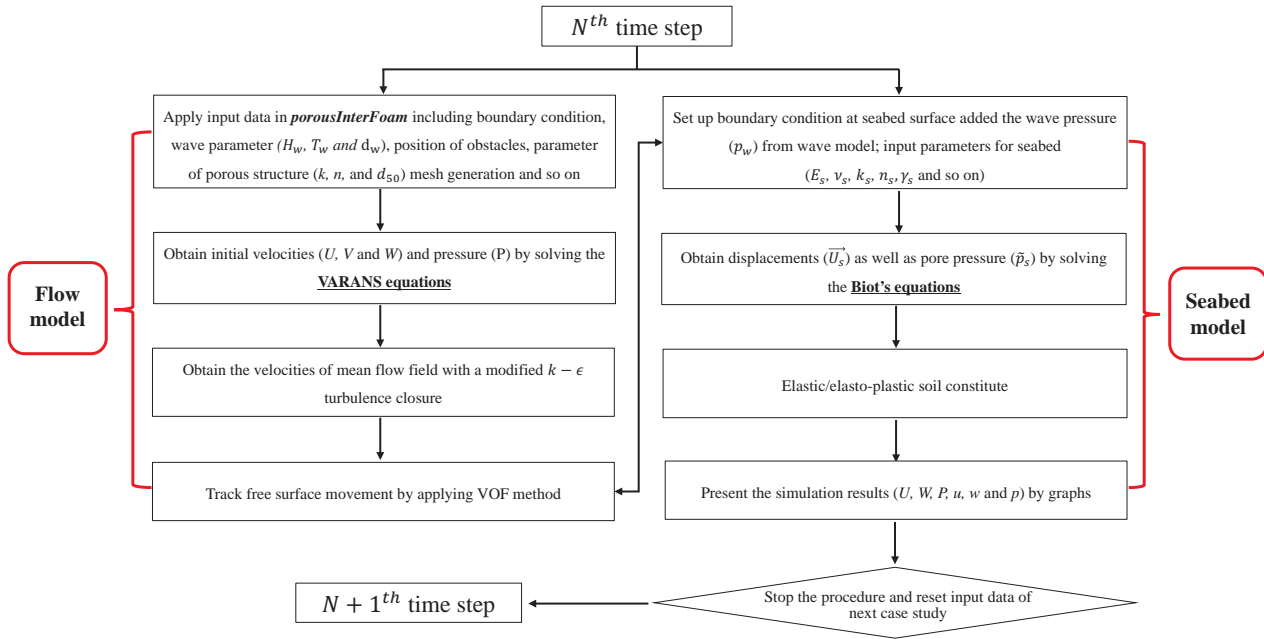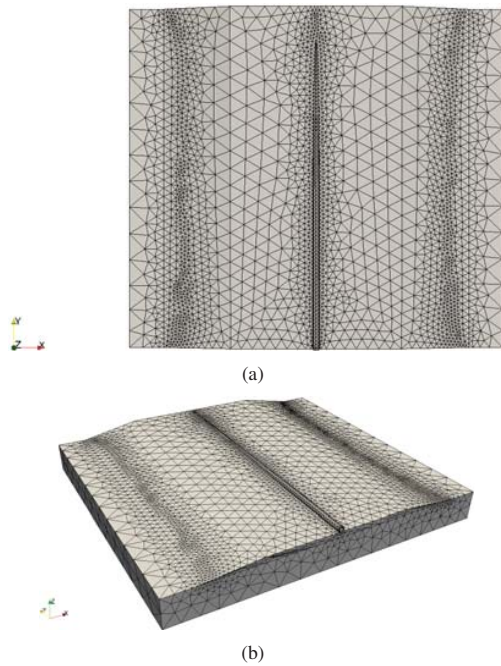
Fig. 2 Numerical scheme of the integrated model

(a)

(b)

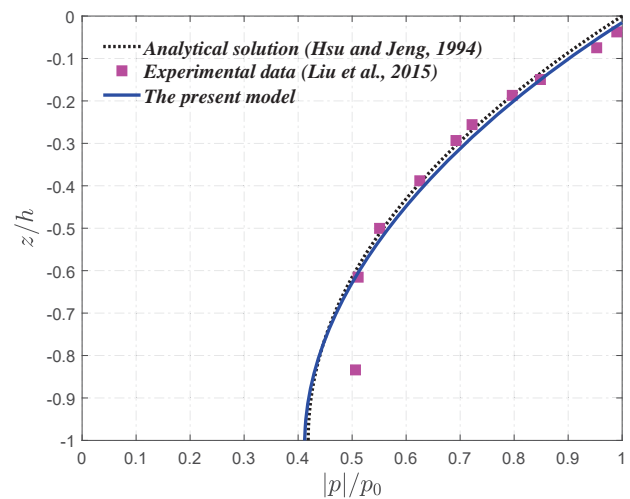Fig. 3 Snapshot of mesh distribution of the present numerical model

Fig. 4 Comparison of the simulated and measured vertical distribution of excess pore pressure against analytical solution [26] and experimental data [29]
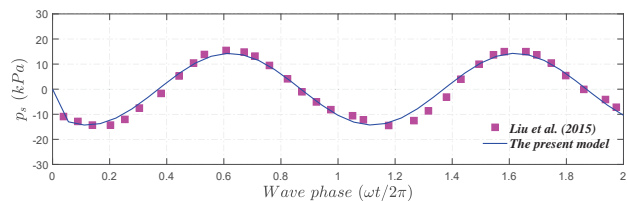

Fig. 5 Comparison of wave-induced pore water pressure between the experimental data [29] at the depth y=-0.067 m (y/h_s=-0.037)

properties of sandy bed and submarine pipeline are listed in Table I unless specified.

A. Flow Model

In this study, a FVM hydrodynamic model based on the VARANS equation is developed in the open-source CFD toolbox OpenFOAM$^{\circledR}$ (version 2.3.0), for investigating the
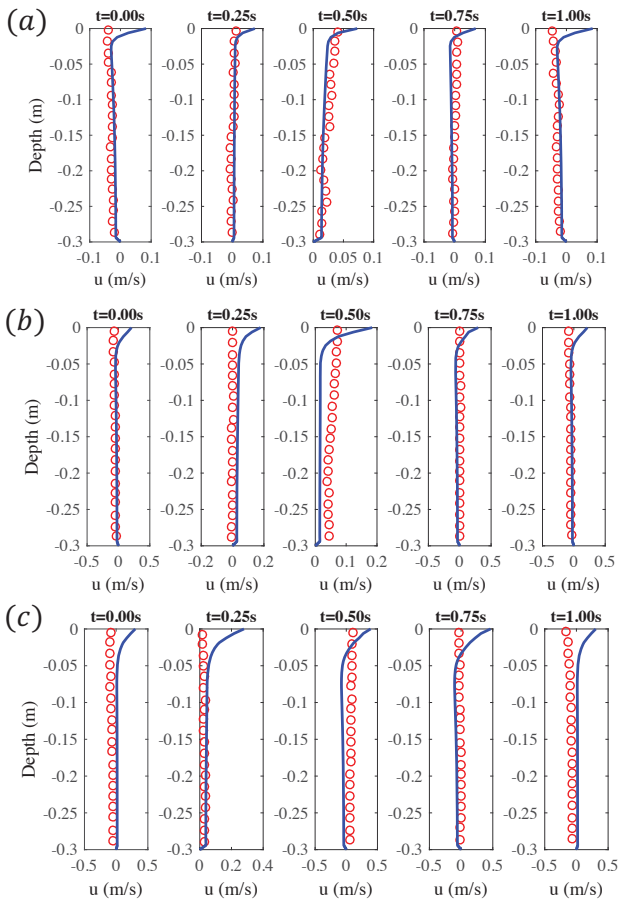
Fig. 6 Validation of horizontal-velocity profiles for wave alone cases against experimental data [30]
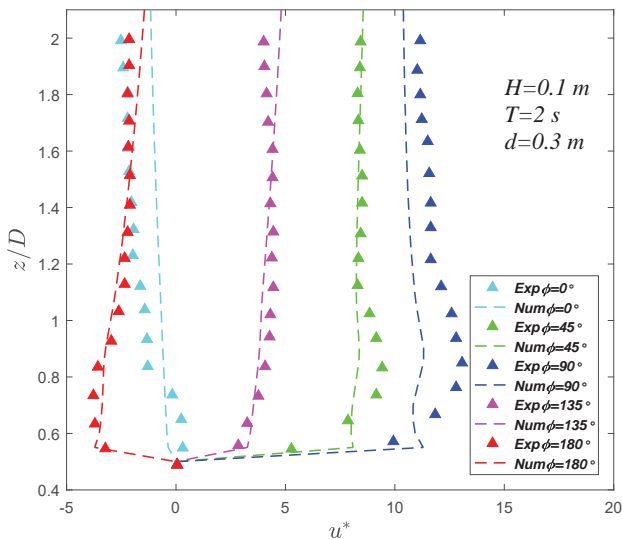

Fig. 7 Validation of Vertical distribution of the dimensionless horizontal fluid velocity through the centre of the pipeline (z/D) for different wave phases against experimental data [31]

wave-submarine pipeline interactions. The modified version of porous interFoam solver (porousInterFoam) is adopted to solve the VARANS equations, using the combined algorithm PIMPLE (which is originated by merging PISO and SIMPLE algorithms) for pressure-velocity coupling. The OlaFoam toolbox [21] is used for the generation/absorption of water waves inside the domain by imposing the water surface elevation and the flow velocity field via a relaxation function. Furthermore, the turbulence effect of the dynamic interaction in the vicinity of the submarine pipeline is considered by addressing the $k - \epsilon$ modelling within the framework of hydrodynamic model. Therefore, the governing equation for simulating the two-phase incompressible flow motion which including the conservation of mass, and conservation of momentum are shown below:

$$\frac{\partial \langle u_i \rangle}{\partial x_i} = 0 \tag{1}$$

$$\frac{\partial \rho \langle u_i \rangle}{\partial t} + \frac{\partial}{\partial x_j}[\frac{1}{n}\rho\langle u_i \rangle \langle u_j \rangle] = -n\frac{\partial \langle p^* \rangle^f}{\partial x_i} + ng_j X_j \frac{\partial \rho}{\partial x_i}$$
$$+ \frac{\partial}{\partial x_j}[\mu_{eff}\frac{\partial \langle u_i \rangle}{\partial x_j}] - [CT] \tag{2}$$

in which U, u_i is the so-called extended averaged or Darcy velocity; n is the porosity, defined as the volume of voids over the total volume; ρ is the density; p^* is the pseudo-dynamic pressure; g is the acceleration of gravity; X is the position vector; μ_{eff} is the efficient dynamic viscosity; u_c is relative velocity field. In terms of the last component in (2), it represents the resistance of the porous media, which is shown:

$$[CT] = a\langle u_i \rangle + b|\langle u \rangle|\langle u_i \rangle + c\frac{\partial \langle u_i \rangle}{\partial t} \tag{3}$$

where the closure term ([CT]) is the hydraulic gradient (proportional to the drop in pressure); the three coefficient (a, b and c) represent the physical properties of the given material, which are calculated based on the theoretical works [22], [23].

B. Seabed Model

The seabed model is constructed under the framework of COMSOL Multiphysics, which is a finite-elements analysis software with an internal solver algorithm and providing the PDE (partial differential equation) modules. In particularly, The quasi-static Biot equation [24] is employed to describe the mechanical behaviour of a hydraulically isotropic porous elastic seabed with appropriate boundary conditions in this study. To save computational effectively, the wave profiles and their corresponding dynamic wave pressure are extracted from the flow model as the surface boundary on the seabed surface, and the outer surface of the submarine pipeline. To avoid the computational error by the reflective waves from the lateral boundary, a large computational domain which is three times of wave length, is applied with fixing two lateral boundaries in the horizontal direction, which has been proved to be sufficient for seabed domain [25].

In general, the soil-pore fluid interaction is determined with Biot's consolidation equation [24], in which the soil skeleton is considered as elastically isotropic material; the pore fluid
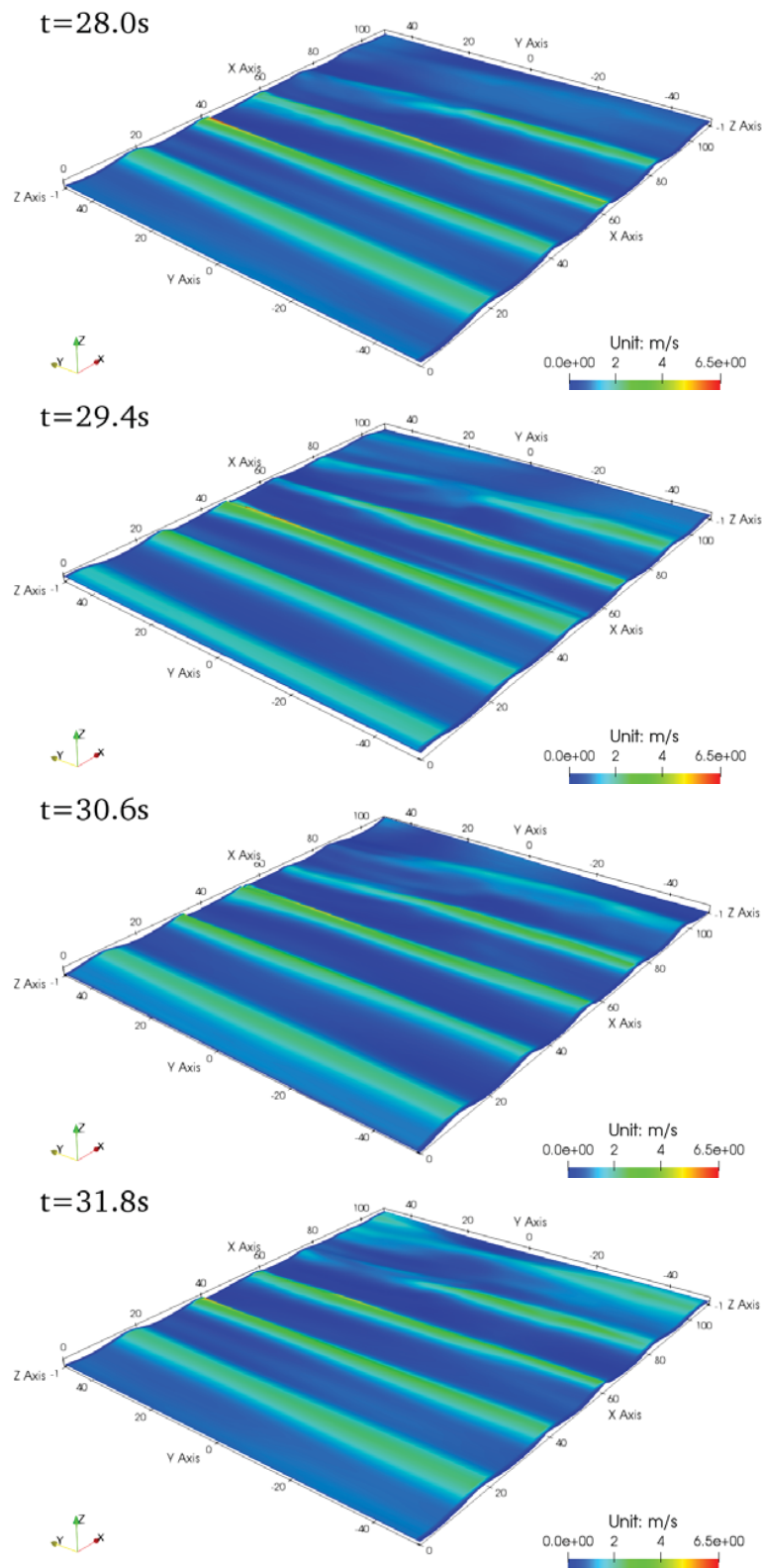
Fig. 8 Time histories of free water surface for the case with a sloping seabed foundation. Note: the surface represent by the value of flow velocity
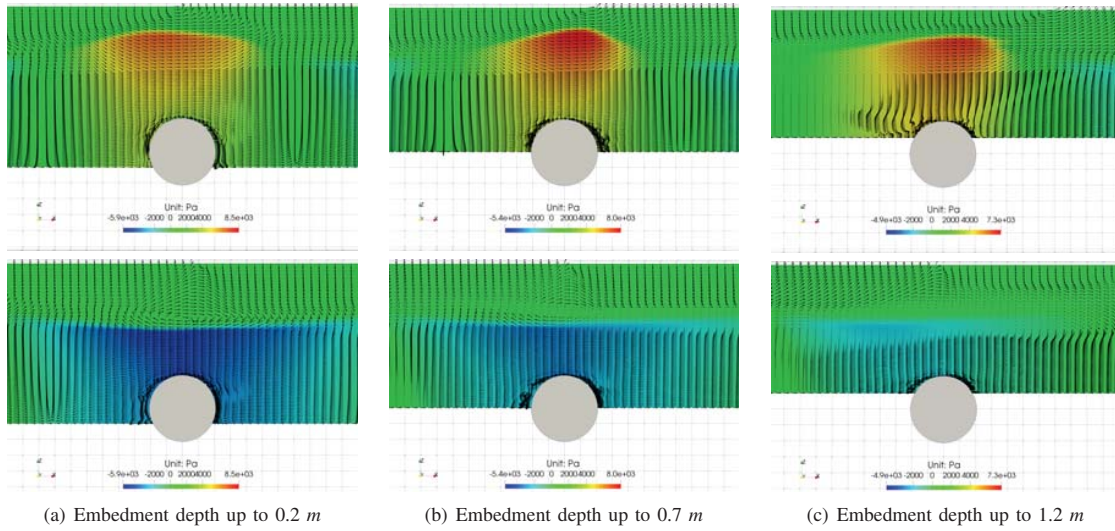
(a) Embedment depth up to 0.2 m (b) Embedment depth up to 0.7 m (c) Embedment depth up to 1.2 m

Fig. 9 The distribution of fluid field for various buried depth (e) in vicinity of the pipeline involving a progressive wave with T_w=4 s and H_w=1 m
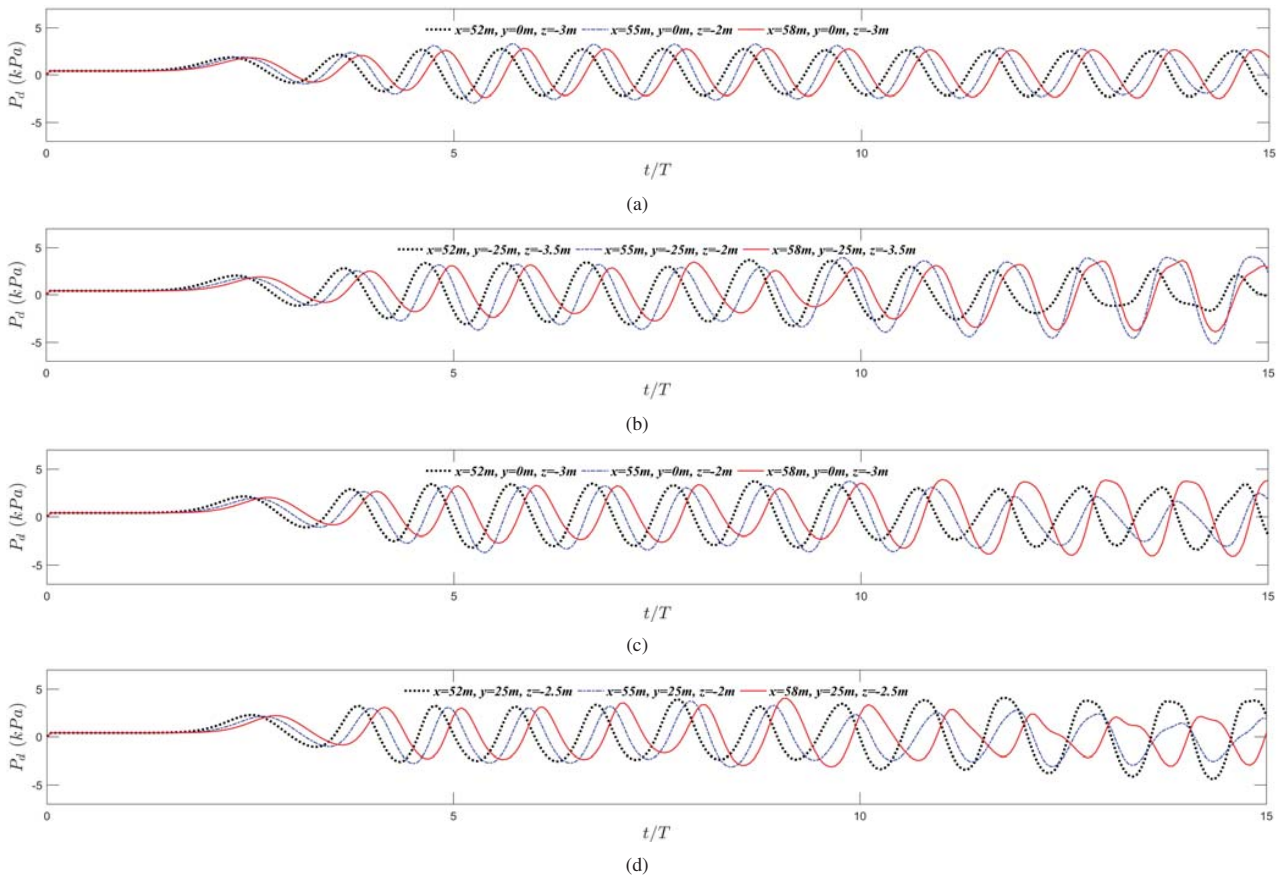

(a)

(b)

(c)

(d)

Fig. 10 Time-varying variation of hydrodynamic pressure at three different locations (Black line: in front of the pipeline; Blue line: on the top of the centre of pipeline; Red line: behind the pipeline) around the submarine pipeline for the specific wave with T_w=4 s and H_w=1 m

(a) σ'_{xx}

(b) σ'_{yy}

(c) σ'_{zz}
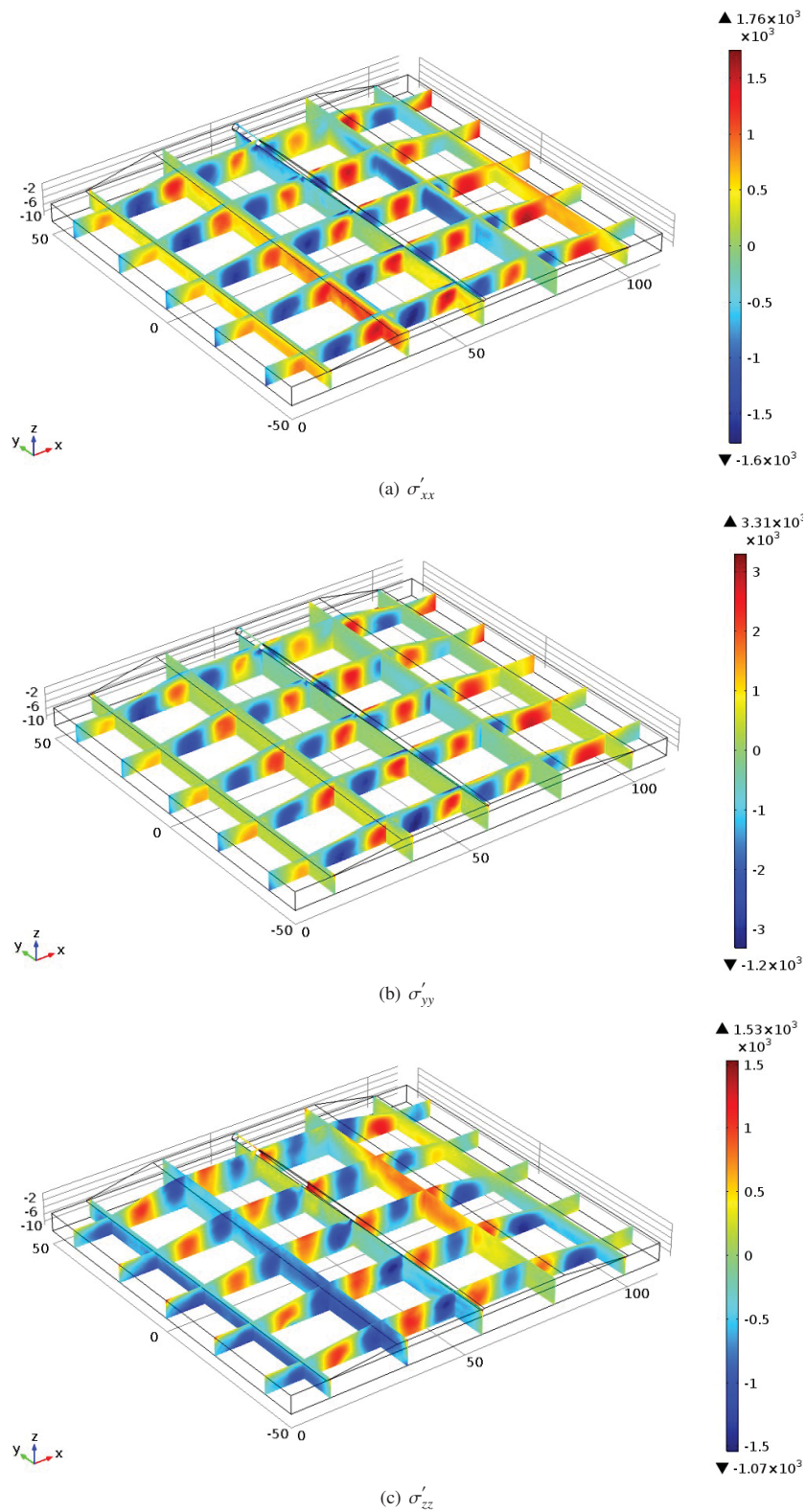
Fig. 11 Distribution of wave-induced dynamic soil response around the buried pipeline for the specific wave with T_w=4 s, H_w=1 m, d_w=6 m, k_s=5.0×10^{-3} m/s and S_r=0.965
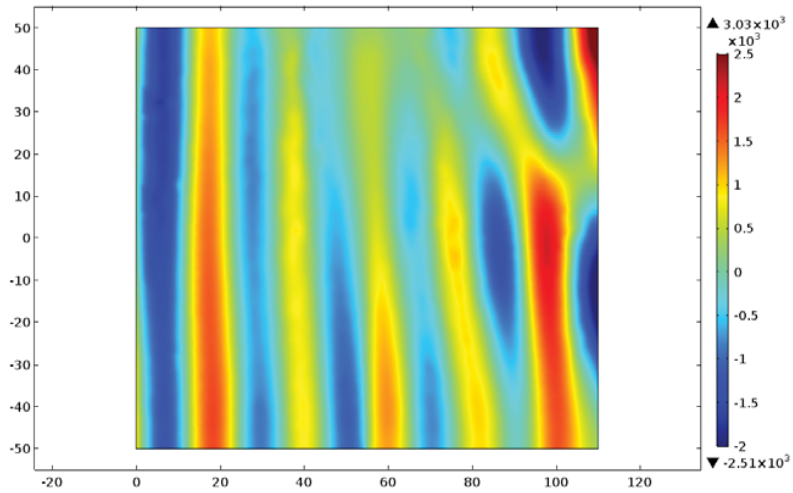
(a) 1:40
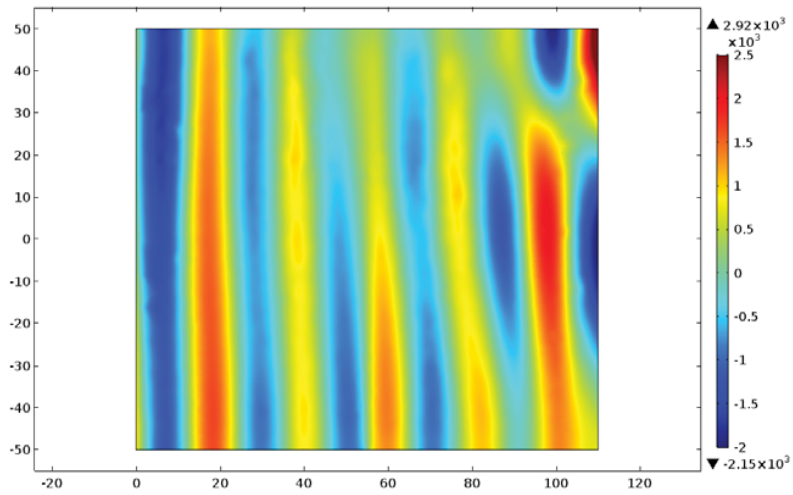
(b) 1:50
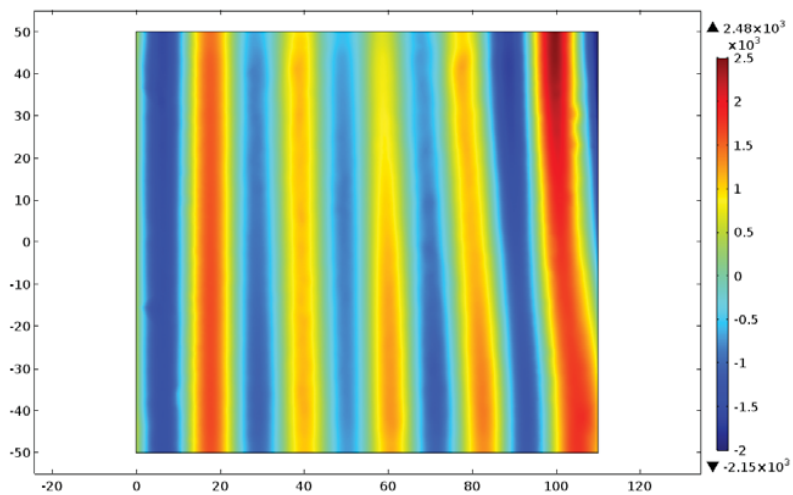
(c) 1:100

Fig. 12 Distribution of wave-induced pore pressure ($\tilde{p}_s$) at XY plane (z=-6.1 m) for the specific wave with T_w=4 s, H_w=1 m, d_w=6 m, k_s= 5.0×10^{-3} m/s and S_r= 0.965
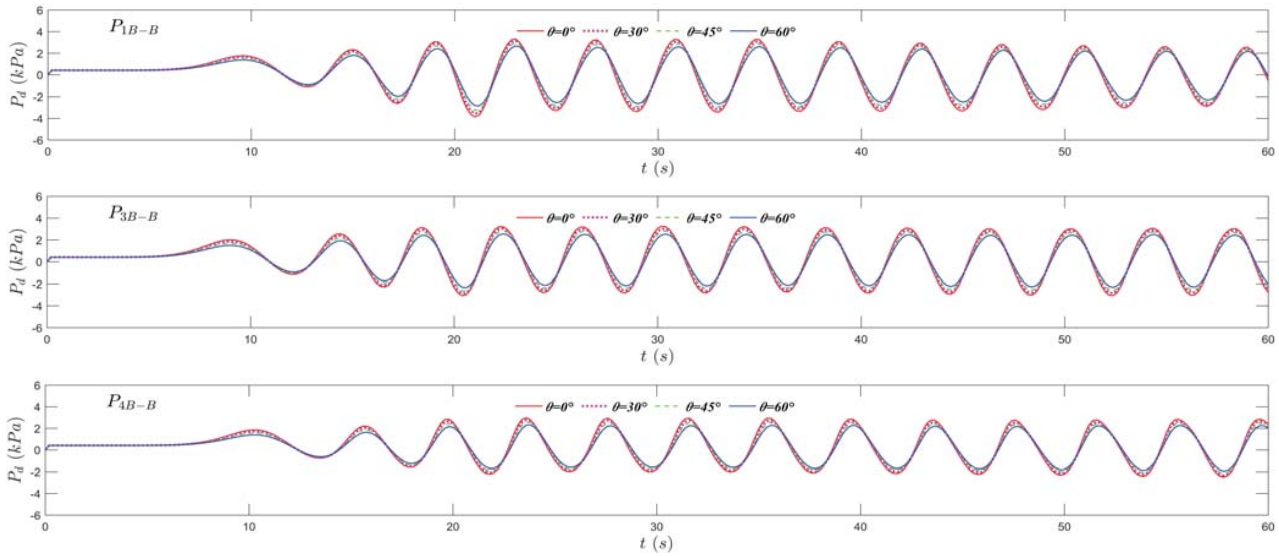
Fig. 13 Time-varying variation of hydrodynamic pressure at three different locations of flat seabed bottom, i.e. (a) in front of the pipeline; (b) on the top of the centre of pipeline; (c) behind the pipeline, which located in section B-B plane for different wave incident angle (T_w=4 s and H_w=1 m)
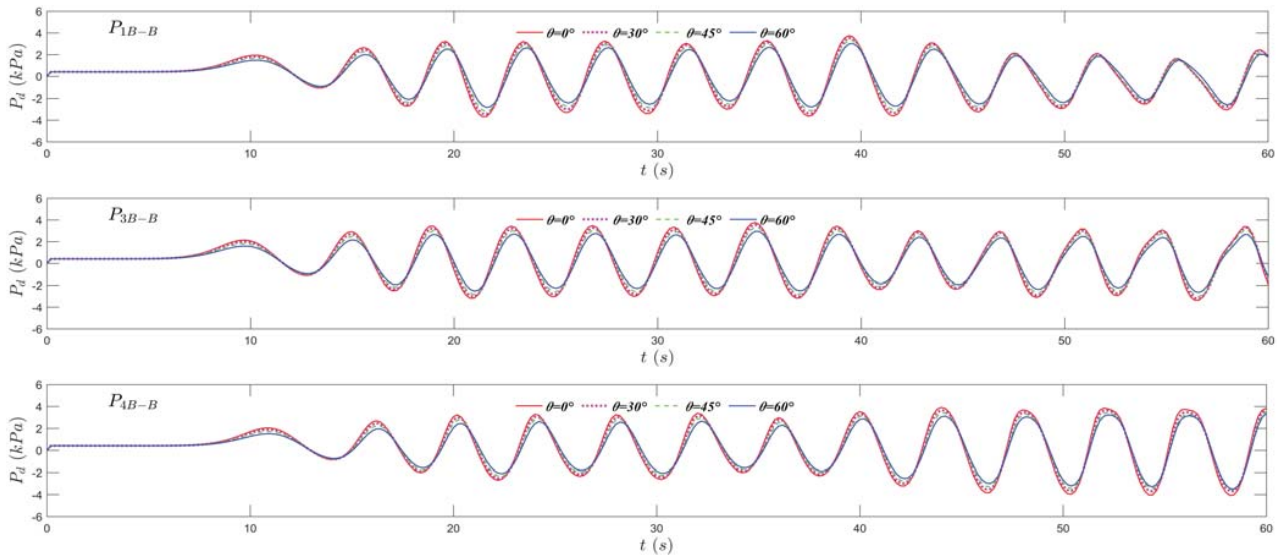

Fig. 14 Time-varying variation of hydrodynamic pressure at three different locations of sloping seabed bottom, i.e. (a) in front of the pipeline; (b) on the top of the centre of pipeline; (c) behind the pipeline, which located in section B-B plane for different wave incident angle (T_w=4 s and H_w=1 m)

is assumed to be compressible and obey Darcy's law, but neglecting the accelerations due to pore fluid and soil motion. For a two-dimensional problem, the government equations can be expressed as

$$\nabla^2 \tilde{p}_s - \frac{\gamma_w n_s \beta_s}{k_s} \frac{\partial \tilde{p}_s}{\partial t} = \frac{\gamma_w}{k_s} \frac{\partial}{\partial t} \left(\frac{\partial u_s}{\partial x} + \frac{\partial v_s}{\partial y} + \frac{\partial w_s}{\partial z} \right), \quad (4)$$

where $\tilde{p}_s$ is the wave-induced pore pressure; γ_w is the unit weight of the pore water; n_s is the soil porosity; ϵ_s is the volume strain defined by

$$\epsilon_s = \frac{\partial u_s}{\partial x_s} + \frac{\partial v_s}{\partial y_s} + \frac{\partial w_s}{\partial z_s} \quad (5)$$

where u_s, v_s and w_s are the soil displacements in the $x-$, $y-$ and $z-$ directions, respectively. And β_s denotes the compressibility of the pore fluid, which is related to the apparent bulk modulus of the pore fluid and the degree of saturation, such that

$$\beta_s = \frac{1}{K_w} + \frac{1 - S_r}{P_{w0}} \quad (6)$$

where K_w is the true bulk modulus of elasticity of water (which may be taken as 1.95×10^9 N/m^2), P_{w0} is the absolute water pressure. When the soil is fully saturated, i.e. it is completely air-free, when $\beta_s = 1/K_w$ since $S_r = 1$.

The equation for overall equilibrium in a porous-elastic

TABLE I
PARAMETERS FOR STUDYING WAVE-SEABED-PIPELINE INTERACTION

Characteristics	Value	Unit
Wave characteristics		
Incident wave height (H_w)	0.6 or various	[m]
Mean water depth (d_w)	6 or 10	[m]
Wave period (T_w)	4 or various	[s]
Soil characteristics		
Permeability (k_s)	$1.0×10^{-1}$ or various	[m/s]
Poisson's ratio (μ_s)	0.35	–
Young's modulus (E_s)	$2×10^7$	[Pa]
Porosity (n_s)	0.425	–
Degree of saturation (S_r)	95 or various	%
Shear modules (G_s)	10^7	[N/m2]
Seabed thickness (h)	10	[m]
Seabed width (W)	110	[m]
Seabed length (L)	100	[m]
Pipeline characteristics		
Young's modulus (E_b)	$2.09×10^{11}$	[Pa]
Pipeline diameter (D)	1.0	[m]
Burial depth (e)	0.2 or various	[m]
Poisson's (μ_p)	0.32	–
Specific weight of pipeline (γ_p)	15	[kN/m^3]

medium, relating to the effective stresses and pore pressure, are given by

$$\frac{\partial \sigma'_x}{\partial x} + \frac{\partial \tau_{xy}}{\partial y} + \frac{\partial \tau_{xz}}{\partial z} = -\frac{\partial \tilde{p}_s}{\partial x}, \quad (7)$$

$$\frac{\partial \tau_{xy}}{\partial x} + \frac{\partial \sigma'_y}{\partial y} + \frac{\partial \tau_{yz}}{\partial z} = -\frac{\partial \tilde{p}_s}{\partial y}, \quad (8)$$

$$\frac{\partial \tau_{xz}}{\partial x} + \frac{\partial \tau_{yz}}{\partial y} + \frac{\partial \sigma'_z}{\partial z} = -\frac{\partial \tilde{p}_s}{\partial z}, \quad (9)$$

where Cauchy stress tensor on the adjacent faces of a two-dimensional stress element consists of two effective normal stresses and shear stress components respectively. The shear stresses are expressed in double subscripts τ_{rs}, defining the stress in the $s-$ direction on a plane perpendicular to $r-$ axis.

Based on the generalized Hookes law, the governing equations for the force equilibrium in the soil can be written as

$$G_s \nabla^2 u_s + \frac{G_s}{(1-2\mu_s)} \frac{\partial \epsilon_s}{\partial x} = -\frac{\partial \tilde{p}_s}{\partial x}, \quad (10)$$

$$G_s \nabla^2 v_s + \frac{G_s}{(1-2\mu_s)} \frac{\partial \epsilon_s}{\partial y} = -\frac{\partial \tilde{p}_s}{\partial y}, \quad (11)$$

$$G_s \nabla^2 w_s + \frac{G_s}{(1-2\mu_s)} \frac{\partial \epsilon_s}{\partial z} = -\frac{\partial \tilde{p}_s}{\partial z}, \quad (12)$$

in which ∇ is the Laplace operator, G_s is shear modulus of soil, which is related to Young's modulus (E) and Poisson's ratio (μ_s) as $E/2(1+\mu_s)$; μ_s is Poisson's ratio.

C. Integration of Flow and Seabed Models

As mention above, several groups of data related to the wave dynamic pore pressure, which calculated in the OpenFOAM, is applied for evaluating the development of soil dynamic behaviors integrated with specific soil characteristics by COMSOL Multiphysics. By consideration of a one-way

coupling process, there are two main steps in the model integration. More precisely, the dynamic wave pressure is extracted from wave model and applied into the seabed model as the boundary condition of top surface through interpolating to the grid points of seabed model at each time step. Afterwards, the seabed model is solved to oscillatory seabed response, including the pore pressure, soil displacement and effective stress. Overall, a working procedure of this integrated numerical model is illustrated in Fig. 2. For the region close to the pipeline, dense mesh is employed as shown in Fig. 3.

III. VERIFICATIONS

To validate the proposed integrated numerical model including both hydrodynamic and geotechnical components, three sets of published laboratory experimental results are used. The wave and soil parameters used in the numerical simulations for comparison are basically the same as those used in the laboratory experiments, unless specified.

A. Comparison with the Analytical Solution and Experimental Data of Pore Pressure $\tilde{p}_s$

As introduced previously, the wave-seabed interaction mechanisms can be described by a set of analytical solutions. Among these, Jeng firstly developed an analytical solution for the wave-induced soil response for an unsaturated anisotropic seabed of finite thickness subject to a three-dimensional wave system [26]. The case with fully saturated isotropic seabed of finite thickness is also available for validation of wave-induced oscillatory soil response without marine structure [27], [28]. Fig. 4 shows the comparison of the maximum pore pressure (P_0) along the depth of seabed between their analytical solutions and the numerical solutions by this present model. As seen, the further comparisons using the experimental data [29] again with the numerical results as depicted in Fig. 5. Overall, these figures clearly show that the computational results of present model for simulating the soil of finite thickness agrees well with both analytical solution and experimental data.

B. Comparison with the Laboratory Measurement of Regular Wave Travelling over a Rigid Bottom

Umeyama conducted a series of experiments to study surface water waves propagating with or without a current in a constant water depth [30]. The experiment was carried out in a recirculating wave tank 25 m long, 0.7 m wide, and 1.0 m deep. A piston-type wave-maker was placed at one end, and a wave absorber was installed at the other end. A pipe under the wave tank was used to recirculate the water flow, generating a steady following current with depth-averaged velocity of U_0=0.08 m/s. During all the tests in the wave tank, the water depth was d=0.3 m and the wave period was T=1.0 s. Tests W1, W2 and W3 were for the waves without the presence of a following current, and their wave heights were 0.0103 m, 0.0234 m and 0.0361 m, respectively. The PIV measurement of horizontal velocity profiles in test W1, W2 and W3 were used in the validation of developed hydrodynamic model for

the wave interaction without porous structures. Details about the laboratory measurement can be referred to [30].

Fig. 6 shows the simulated and measured horizontal velocity profiles at various phase values involved in the wave interactions. For all three cases, the simulated velocity data appear to be in reasonable accord with those obtained by the PIV measurement in the wave tank. It was found that the velocity profile is significantly affected by the surface wave motion, and an upward-directed velocity gradient can be observed when wave trough arrives.

C. Comparison with Laboratory Investigation of the Nearbed Dynamic Interaction between Regular Wave and the Submarine Pipeline

Mattioli carried out sets of experiment to investigate the near-bed dynamics around a submarine pipeline laying on different types of seabed. The experiments at the basis of their study were performed in a wave flume 50 *m* long, 1.3 *m* high and 1 *m* wide. The regular wave was generated by the piston-type wave-maker and propagated toward the model section, which was 1.5 *m* long and placed approximately 10 *m* seaward of the porous bed and about 15 *m* shoreward of the generation system. Within the model section, a plexiglass pipe of 5 *cm* diameter and 1 *m* length was fastened to the wall of the flume, which was normal to the wave direction with an initial embedment e/D=0. Also, four wave gauges were used to measure the variation of water surface during the experimental process. In particular, two of them, (i.e. S3 and S4) were placed at the seaward and shoreward end of the model section separately. Regarding to wave condition, The local water level was fixed with h=0.3 *m*. Other than that, the wave height H was 0.1 *m* and wave period T=2 *s* (alternatively, KC=13.67, Re=1.7E+0.4 and Ur=38.93) for capturing the best description of both the flow and sand particles motion. Meanwhile, the PTV measurements was used to characterize the flow in the surroundings of the submarine pipeline together with an Acoustic Doppler Velocimetry (ADV) with the aim to calibration and validation. As for the bottom of the flume, it was made of well-sorted sand with a mean diameter D_{50}=0.6 *mm* which can be considered as an erodible seabed.

Fig. 7 shows the vertical distribution of the dimensionless horizontal fluid velocity (u^*) through the centre of the pipeline (z/D) for different wave phases from 0° to 180° with a increment of 45°. The dimensionless velocity (u^*) is equal to $u/(H/T)$, and D is the diameter of the submarine pipeline. Overall, the numerical results show that the present wave model agree with the experimental data [31].

IV. RESULTS AND DISCUSSIONS

In this section, the validated model is applied to investigate the response of the seabed and a submarine pipeline under progressive wave loading in real offshore environment. Here, three typical sections (i.e. *XZ* plane) are considered to precisely investigate the physical process involved in the wave-seabed-structure interactions around the submarine pipeline. Moreover, four different reference points are used to evaluate the hydrodynamic wave pressure above seabed and

the distribution of wave-induced soil response along depth, where P_1 and P_2 are located on the top and the bottom of the pipeline separately. For the rest of two reference points, i.e. P_3 and P_4, which are located at the seaward and shoreward edge of the buried pipeline, respectively. All of the wave characteristics and properties of sandy seabed are listed in Table I unless specified.

A. Wave Profiles

The main hydrodynamic function of a submarine pipeline is to transport a variety of gasses and fluids to inshore region from the offshore platform owing to the significant growth over the past decades. In this section, we will further consider the existence of sloping seabed and investigate its influence on the local hydrodynamic process in the vicinity of the submarine pipeline using the developed hydrodynamic model. As depicted in Fig. 8, a porous seabed with a slope of 1 : 50 can significantly influences the variation of free water surface with respect to time. More precisely, Fig. 8 shows the time-varying distribution of flow velocity on the free water surface during a wave period (T_w=4 *s*). It is found that, the flow can obtain high velocity in front of the submarine pipeline where the water depth (d_w) becomes smaller gradually.

In general, the flow pattern can be altered by surrounding geometry intermediately. In this study, the burial depth of submarine pipeline (e) is determined from its bottom to the surface of mudline. To illustrate, the embedment depth of the submarine pipeline is gradually increasing as the increase of slope gradient. Fig. 9 shows the distribution of flow velocity in the vicinity of buried pipeline for different embedment depth. As seen, a larger zone with high density flow vector is observed at the plane located at y=-25 *m*, where the embedment depth of pipeline (e) is 0.2 *m*. In other words, more intensive interaction of wave is generated, then quickly propagating toward the adjacent marine structure. Whereas the large embedment depth is not seem to largely block fluid motion into the downstream of the submarine pipeline since the fluid motion keeps moving with the direction which is close to be parallel to the seabed surface. Regarding to the buried depth at the other two planes, the vortex structure (i.e. flow separation or vortex movement) is easily occurred in the neighbourhood region during the whole wave propagating process.

B. Hydrodynamic Process Involved in the Wave-Submarine Pipeline Interactions

To study the hydrodynamic process in vicinity of submarine pipeline, a total of nine reference locations of three disparate sections around its neighbourhood region are incorporated as depicted in Fig. 10. It is noted that, each graph has three different lines to represent the hydrodynamic pressure with respect to time of the corresponding locations. The first figure clearly demonstrate the time histories of hydrodynamic pressure related to a simple numerical case in which a submarine pipeline is laid on the flat porous seabed. Regrading to that, we only investigate the section B-B since the a flat seabed will not induce a three dimensional phenomenon of
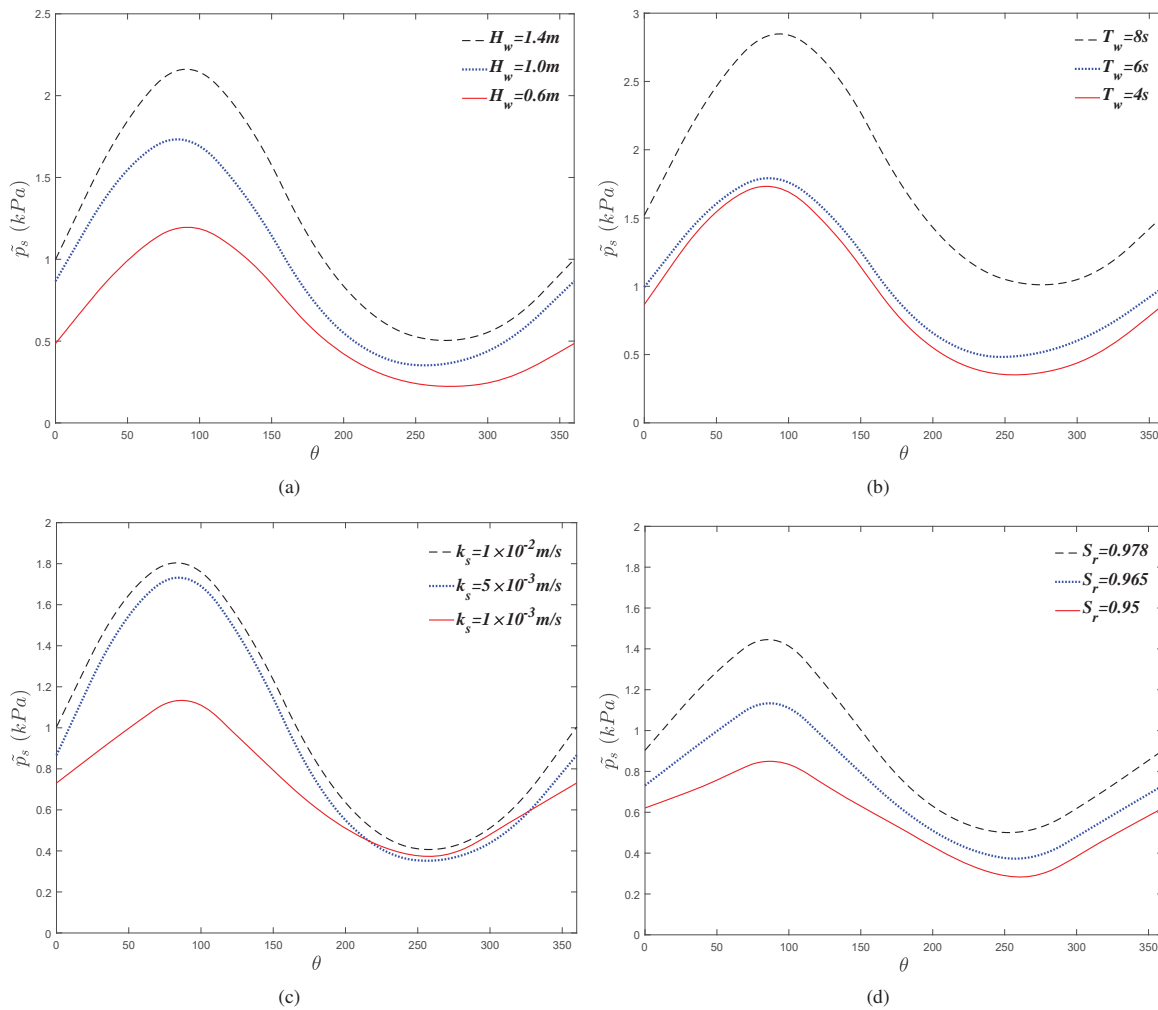
Fig. 15 Distribution of oscillatory pore pressure ($\tilde{p}_s$) along the periphery of the pipeline under the wave trough loading for various values of (a) wave height; (b) wave period; (c) soil permeability; (d) degree of saturation

wave field. However, in terms of the case study involving a sloping seabed, the historical variation of hydrodynamic pressure of three sections are presented.

As seen, compared to the case involving a flat seabed foundation (see Fig. 10 (a)), the case where wave and sloping seabed interaction simultaneously with a submarine pipeline yield significant difference in the hydrodynamic pressure around the structure, which may in turn result in the variation in the wave-induced geotechnical components in the seabed foundation. It is noted that, the variation of hydrodynamic pressure is discussed in the specific region starting from $y=-25$ m to 25 m. To illustrate, the existence of sloping seabed along the $y-$ direction could significantly increase the amplitude of hydrodynamic force in front of the submarine pipeline and making the fluid-structure interaction become more intensive. On the contrary, the wave amplitude acting on the location where is behind the submarine pipeline decrease along the direction fo slope gradient of seabed where there is larger burial depth. This may contribute to the fact that the incoming

wave is no longer becoming stable as a result of breaking wave. In other words, a new wave pattern appears after the interaction among the wave, sloping seabed and structure, and continuously affects the geotechnical components in the rear area of interest.

C. Wave-Induced Seabed Response around the Submarine Pipeline

The pipelines are either laid on the seabed or buried inside trenches that are either pre-cut or formed during laying processes. Burying the pipelines into seabed diminishes hydrodynamic wave forces acting on them and avoids unexpected damage induced by finishing and trawling activities. Taking the wave-induced pressure acting on the sand bed and on the submarine pipeline as the surface pressure boundary conditions, the dynamics of the pipeline and its seabed foundation is investigated numerically using the developed model in three dimensional space. As introducing previously, a sloping seabed is considered here
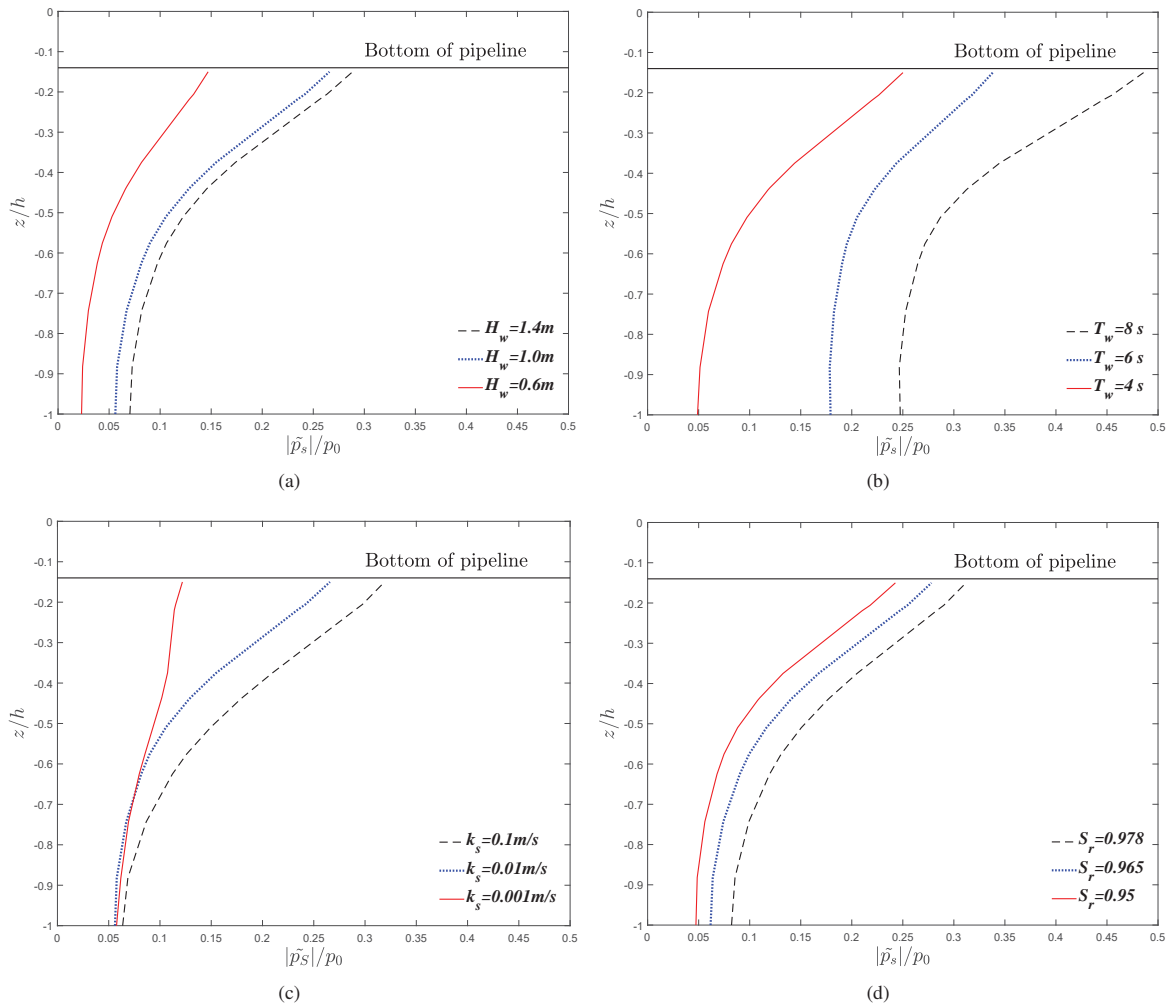
Fig. 16 Distribution of oscillatory pore pressure ($\tilde{p}_s$) along the vertical line through the centre of the pipeline under the wave trough loading for various values of (a) wave height; (b) wave period; (c) soil permeability; (d) degree of saturation

for investigating the effect of irregular geometry on the distribution of wave-induced seabed response including the pore pressure and effective stress as indicated in Fig. 11. As seen, the soil is compressive with negative value whereas it is tensile represented by positive value in the region where large amplitude of pore pressure existing.

Fig. 12 demonstrates that distribution of wave-induced oscillatory response for different slope gradient at the bottom plane, which is beneath the submarine pipeline and located at z=-6.1 m. It is found that, the slope gradient of the porous seabed indeed has significant effect on the distribution of wave-induced soil oscillatory pressure in the seabed foundation around the submarine pipeline. As seen, The zones with large amplitude of wave-induced pressure distribute alternately in the specific region behind the submarine pipeline where the wave-induced soil liquefaction can be easily happened.

D. Effect of Wave Direction on hydrodynamic force around the submarine pipeline

Figs. 13 and 14 show wave-induced dynamic pressure acting on the seabed and the structure at three typical locations for different wave incident angle among 0°, 30°, 45° and 60° in the case studies with flat seabed and sloping seabed, respectively. For evaluating the effect of wave incident angle, we only investigate the variation of hydrodynamic pressure at three typical locations of the *XZ* plane which located at *y*=0 *m* (section B-B). It is pointed out that the wave incident angle (ϕ) is defined as the intersection angle between the direction of progressive wave and *x*− axis.

As seen, the influence of wave direction on the amplitude of hydrodynamic pressure is slightly significant compared to the effect of slope gradient (α). More precisely, the larger amplitude of hydrodynamic pressure can be detected with a wave incident angle of 0° in which a progressive wave with perpendicular direction towards the submarine pipeline. Thereafter, the decrease of wave incident angle can induce
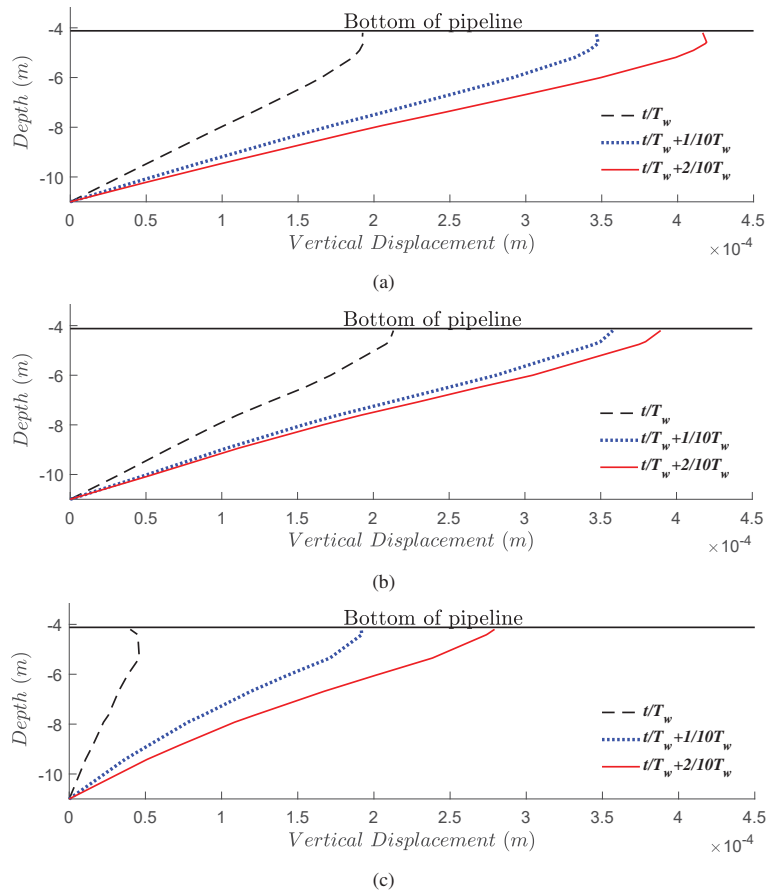
Fig. 17 Time-varying distribution of vertical displacement through the centre of the pipeline under the wave trough loading at (a) x=-25 m; (b) x=0 m; (c) x=25 m with T_w=4 s, H_w=1 m, d_w=6 m, k_s=5.0×10^{-3} m/s and S_r=0.965

larger amplitude of wave pressure on the three typical locations including P_1, P_3 and P_4 around the submarine pipeline in terms of the case involving both flat and sloping seabed. However, a sloping seabed could alter the distribution of wave force with the passage of time after the 10th wave period (T=4 s). This is likely attributed to the transformation of wave flow pattern by the sloping geometry.

E. Oscillatory Pore Pressure along the Periphery of Submarine Pipeline

In this section, the results of oscillatory pore pressure along the surface ($0°< \theta < 360°$) of the submarine pipeline is presented, as shown in Figs. 15 (a)-(c). The maximum value of $\tilde{p}_s$ can be found in the location (θ=90°) which is in the surrounding region of seabed surface, whereas the minimum value is located at the bottom of the pipeline (θ=270°). This implies that, the soil liquefaction is more likely to occur in the upper region along the pipeline. Additionally, there is a slight difference can be obtained in the upper-half and down-half surface with respect to θ=90° and θ=270°, respectively. This is may be attributed to non-linear effect of sloping seabed as a result in the asymmetrical distribution of $\tilde{p}_s$ along the both upper and lower part of pipeline.

Figs. 15 (a)-(d) reveal the effects of wave height (H_w), wave period (T_w), soil permeability (k_s) and degree of saturation (S_r) on the distribution of $\tilde{p}_s$ along the periphery of pipeline. According to the figures, the amplitude of $\tilde{p}_s$ is observed to be increasing as the increase of H_w, T_w, k_s and S_r. In particular, the effect of wave period (T_w) and soil permeability (k_s) are more significant than the others. Moreover, the direct influence of H_w, T_w, k_s and S_r on the distribution of $\tilde{p}_s$ is more important in the region of upper part of pipeline compared to that in the vicinity of bottom of pipeline.

F. Vertical Distribution of Oscillatory Pore Pressure and Soil Displacement

Figs. 16 (a)-(d) show the variation of $\tilde{p}_s$ through the central line of pipeline under the wave trough loading for various value of H_w, k_s and S_r. More precisely, the bottom of pipeline at three plane are both located at z/h=-0.14. To study the above effects, the case study involving variation of $\tilde{p}_s$ at XZ plane located at y=0 m is conducted here. As illustrate from these figs, it is found that, the magnitude of $\tilde{p}_s$ has a positive relationship with H_w, T_w, k_s and S_r. Besides, the value of $\tilde{p}_s$ is gradually attenuated as increase of depth to bottom. In comparison with other effect on vertical distribution of $\tilde{p}_s$, the
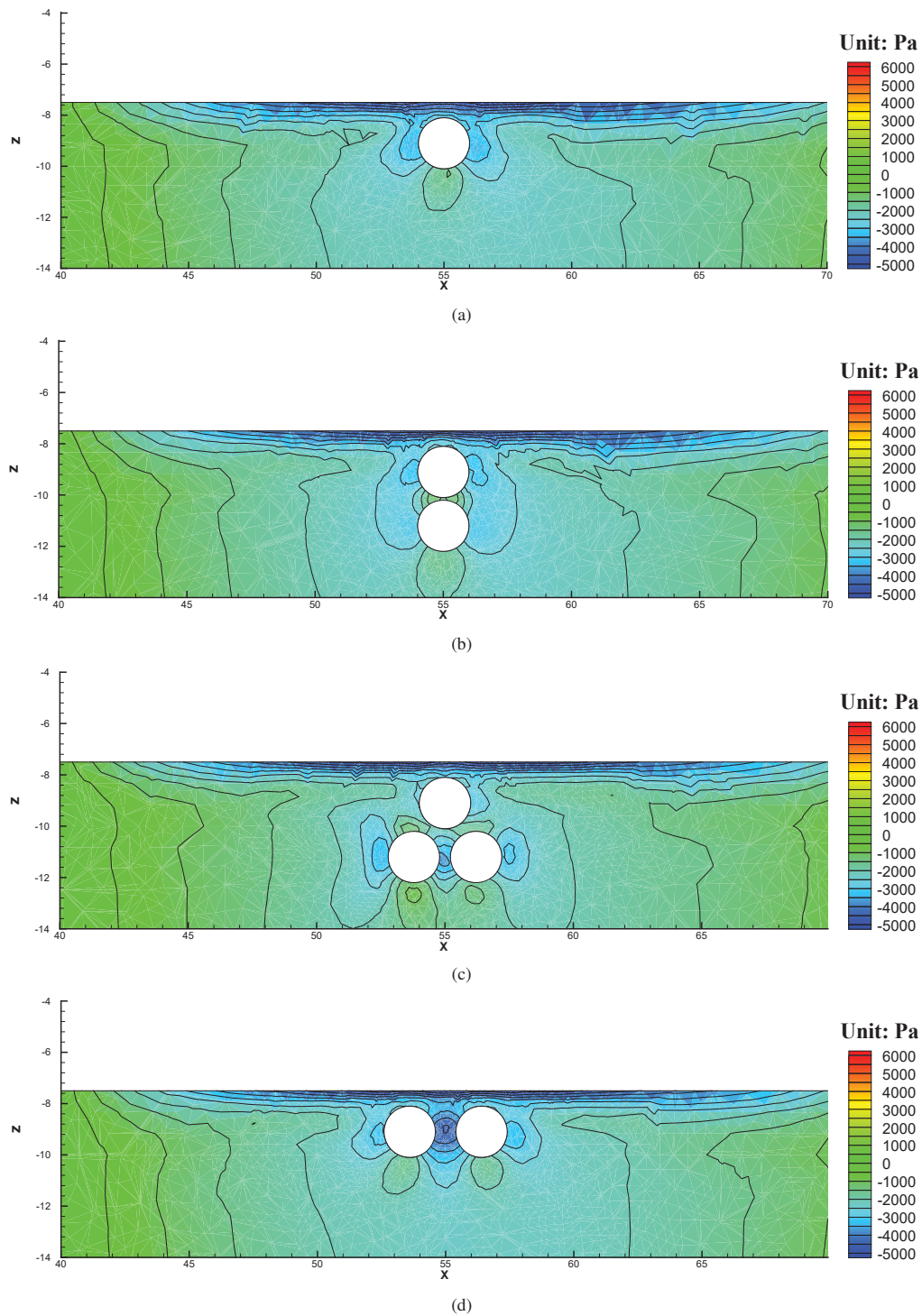
(a)

(b)

(c)

(d)

Fig. 18 Distribution of wave-induced pore pressure ($\tilde{p}_s$) for various cases involving group of submarine pipelines in which T_w=8 s, H_w=1.6 m, d_w=10 m, k_s= 1.0×10^{-4} m/s and S_r= 0.965

soil permeability (k_s) seem to be more significant in the top 50% of depth below the bottom of pipeline. A seabed with relatively small magnitude of k_s, the vertical variation of $\tilde{p}_s$ is more steeper as a result in weak uplift force on the pipeline.

Figs. 17 (a)-(c) shows the variation of vertical displacement through the centre of pipeline during the pass of wave trough loading at three separate sections as mention above. As revealed by these figures, the soil deformation at different locations are experienced inequable wave loading. As can be expected, the largest gradient of u_z within the 3/10 T_w can be obtained at location x=-25 m where there is deeper water depth inducing a larger wave pressure. Moreover, the embedment of pipeline (e) here is relatively small compared to other two regions. Therefore, less thickness of e can not offer enough protection for the stability of pipeline owing to the flow can easily penetrate into its lower foundation with high soil permeability (k_s) in a sandy seabed.

G. Effect of Group Pipes on Pore Pressure

As reported before, the submarine pipeline is applied to transport the natural gas and oil between the inland and offshore area for the purpose of increasing industrial development. Thereafter, group of submarine pipeline is necessary to be designed and installed for achieving its multifunction rather than one single burial pipeline. Consequentlya better understanding of stability of group pipeline is vital for coastal engineers when they involved in the design project of marine structure. Fig. 18 show the distribution of pore pressure in the porous seabed for the cases with one single and group of submarine pipeline, respectively. As seen, the wave-induced dynamic pressure instantly penetrated into the specific soil layer above the submarine pipeline. It is also noted that, the amplitude of transient pore pressure with the area between two adjacent is larger than that of its lateral side where there are more than one submarine pipeline in the horizontal direction (see Figs. 18 (c)-(d)).

V. Conclusion

In this study, a 3-D integrated model is developed to investigate the the interaction between the wave, seabed and submarine pipeline. In this present study, the soil model is developed with FEM method by solving the classical Biot's consolidation equation (QS model); the wave model is simulated by solving the Navier-Stokes equation under the framework of FVM method. The developed model is well validated through comparison with a series of laboratory experiments. Based on the numerical results, the following conclusions can be drawn:

1) Despite there is no available three dimensional experiment involving wave-pipeline-seabed interaction for validation, a comprehensive comparison between he present numerical model against the 2D analytical solution and experimental data is conducted. The comparison indicates that the present model is reliable for the evaluation of wave-induced transient pore pressure in the vicinity of the submarine pipeline.

2) The wave motions are significantly affected by the gradient of slope seabed foundation. Numerical results indicate that a larger slope along the longitude of submarine pipeline can induce a discontinuous distribution of wave-induced transient pore pressure. For this reason, the buried pipeline is undertaken different kind of external forces from ocean wave and surrounding seabed foundation, respectively.

3) The wave-induced transient pore pressure can increase to a large value in the case of porous seabed with high permeability and degree of saturation subject to loading induced by large amplitude wave height and longer wave period. Moreover, based on the numerical results, the wave-induced transient pore pressure along the upper part of buried pipeline is larger than that of lower part of pipeline.

References

[1] A. C. Palmer and R. A. King, *Subsea pipeline engineering*. PennWell Books, 2004.
[2] B. M. Sumer, F. H. Dixen, and J. Fredsøe, "Cover stones on liquefiable soil bed under waves," *Coastal Engineering*, vol. 57, no. 9, pp. 864–873, 2010.
[3] J. Fredsøe, "Pipeline–seabed interaction," *Journal of Waterway, Port, Coastal, and Ocean Engineering*, vol. 142, no. 6, p. 03116002, 2016.
[4] B. M. Sumer, *Liquefaction around marine structures*. World Scientific, 2014.
[5] K. Zen and H. Yamazaki, "Field observation and analysis of wave-induced liquefaction in seabed," *Soils and Foundations*, vol. 31, no. 4, pp. 161–179, 1991.
[6] H. B. Seed and M. S. Rahman, "Wave-induced pore pressure in relation to ocean floor stability of cohesionless soils," *Marine Geotechnology*, vol. 3, no. 2, pp. 123–150, 1978.
[7] T. Yamamoto, "Wave-induced pore pressures and effective stresses in inhomogeneous seabed foundations," *Ocean Engineering*, vol. 8, pp. 1–16, 1981.
[8] O. S. Madsen, "Wave-induced pore pressures and effective stresses in a porous bed," *Géotechnique*, vol. 28, no. 4, pp. 377–393, 1978.
[9] B. M. Sumer, J. Fredsøe, S. Christensen, and M. L. Lind, "Sinking/floatation of pipelines and other objects in liquefied soil under waves," *Coastal Engineering*, vol. 38, pp. 53–90, 1999.
[10] B. M. Sumer, C. Truelsen, T. Sichmann, and J. Fredsøe, "Onset of scour below pipelines and self-burial," *Coastal engineering*, vol. 42, no. 4, pp. 313–335, 2001.
[11] T. C. Teh, A. C. Palmer, and J. S. Damgaard, "Experimental study of marine pipelines on unstable and liquefied seabed," *Coastal Engineering*, vol. 50, pp. 1–17, 2003.
[12] C. Zhou, G. Li, P. Dong, J. Shi, and J. Xu, "An experimental study of seabed responses around a marine pipeline under wave and current conditions," *Ocean Engineering*, vol. 38, no. 1, pp. 226–234, 2011.
[13] D. Jeng and Y. Lin, "Wave–induced pore pressure around a buried pipeline in gibson soil: finite element analysis," *International Journal for Numerical and Analytical Methods in Geomechanics*, vol. 23, no. 13, pp. 1559–1578, 1999.
[14] D.-S. Jeng and L. Cheng, "Wave-induced seabed instability around a buried pipeline in a poro-elastic seabed," *Ocean Engineering*, vol. 27, no. 2, pp. 127–146, 2000.

[15] A. H. D. Cheng and P. L.-F. Liu, "Seepage force on a pipeline buried in a poroelastic seabed under wave loading," *Applied Ocean Research*, vol. 8, no. 1, pp. 22–32, 1986.

[16] F. Gao, D. S. Jeng, and H. Sekiguchi, "Numerical study on the interaction between non-linear wave, buried pipeline and non-homogenous porous seabed," *Computers and Geotechnics*, vol. 30, no. 6, pp. 535–547, 2003.

[17] F.-P. Gao and Y.-X. Wu, "Non-linear wave induced transient response of soil around a trenched pipeline," *Ocean Engineering*, vol. 33, pp. 311–330, 2006.

[18] X.-L. Zhou, D.-S. Jeng, Y.-G. Yan, and J.-H. Wang, "Wave-induced multi-layered seabed response around a buried pipeline," *Ocean Engineering*, vol. 72, pp. 195–208, 2013.

[19] Z. Lin, Y. Guo, D.-s. Jeng, C. Liao, and N. Rey, "An integrated numerical model for wave–soil–pipeline interactions," *Coastal Engineering*, vol. 108, pp. 25–35, 2016.

[20] H.-Y. Zhao, D.-S. Jeng, Z. Guo, and J.-S. Zhang, "Two dimensional model for pore pressure accumulations in the vicinity of a buried pipeline." *Journal of Offshore Mechanics and Arctic Engineering, ASME*, vol. 136(4), p. 042001, 2014.

[21] P. Higuera, J. Lara, and I. Losada, "Realistic wave generation and active wave absorption for vavier-stokes models: Application to openfoam," *Coastal Engineeirng*, vol. 71, pp. 102–118, 2013.

[22] F. Engelund, *On the laminar and turbulent flows of ground water through homogeneous sand*.   Akad. for de Tekniske Videnskaber, 1953.

[23] H. Burcharth and O. Andersen, "On the one-dimensional steady and unsteady porous flow equations," *Coastal engineering*, vol. 24, no. 3-4, pp. 233–257, 1995.

[24] M. A. Biot, "General theory of three-dimensional consolidation," *Journal of Applied Physics*, vol. 26, no. 2, pp. 155–164, 1941.

[25] J. Ye and D.-S. Jeng, "Response of seabed to natural loading-waves and currents," *Journal of Engineering Mechanics, ASCE*, vol. 138, no. 6, pp. 601–613, 2012.

[26] J. R. C. Hsu and D.-S. Jeng, "Wave-induced soil response in an unsaturated anisotropic seabed of finite thickness," *International Journal for Numerical and Analytical Methods in Geomechanics*, vol. 18, no. 11, pp. 785–807, 1994.

[27] D. Jeng and J. Hsu, "Wave-induced soil response in a nearly saturated sea-bed of finite thickness," *Geotechnique*, vol. 46, no. 3, pp. 427–440, 1996.

[28] D.-S. Jeng, *Porous Models for Wave-seabed Interactions*.   Springer, 2012.

[29] B. Liu, D.-S. Jeng, G. Ye, and B. Yang, "Laboratory study for pore pressures in sandy deposit under wave loading," *Ocean Engineering*, vol. 106, pp. 207–219, 2015.

[30] M. Umeyama, "Coupled piv and ptv measurements of particle velocities and trajectories for surface waves following a stedy current," *Journal of Waterway, Port, Coastal and Ocean Engineering , ASCE*, vol. 137, pp. 85–94, 2011.

[31] M. Mattioli, J. M. Alsina, A. Mancinelli, M. Miozzi, and M. Brocchini, "Experimental investigation of the nearbed dynamics around a submarine pipeline laying on different types of seabed: the interaction between turbulent structures and particles," *Advances in water resources*, vol. 48, pp. 31–46, 2012.

Dong-Sheng Jeng is the Professor who has been working in the areas of offshore geotechnics, coastal/ocean engineering, groundwater hydraulics, artificial neural networks, renewable marine energy and plant science. He employs various analytical and numerical techniques to obtain theoretical understanding of his research problems and applied to engineering practice.

Zuodong Liang is a PhD student studying offshore geotechnics engineering in the School of Engineering at Griffith University. Currently, he works on the numerical investigation of three-dimensional model for seabed instability around offshore pipelines under ocean wave loading.